Optical design of a thin curved lightguide and manufacturing using ophthalmic approaches

Ozan Cakmakci, Oscar A. Martinez, Jerry Carollo

Ozan Cakmakci, Oscar A. Martinez, Jerry Carollo, "Optical design of a thin curved lightguide and manufacturing using ophthalmic approaches," Proc. SPIE 11062, Digital Optical Technologies 2019, 110620H (21 June 2019); doi: 10.1117/12.2530526

SPIE.

Event: SPIE Digital Optical Technologies, 2019, Munich, Germany

Invited Paper

Optical Design of a Thin Curved Lightguide and Manufacturing Using Ophthalmic Approaches

Ozan Cakmakci, Oscar A. Martinez, and Jerry Carollo

Google LLC, 1600 Amphitheater Parkway, Mountain View, CA 94043

ABSTRACT

We present an underexplored variation of the classical optical freeform prism design that incorporates 3 optical surfaces. This optical architecture can make use of one, two, or three freeform surfaces. Our initial prototype uses a single freeform surface along with a sphere and a flat surface to simplify manufacturing complexity. There are two key contributions in this paper that to our knowledge have not been achieved previously: 1) the design of a thin, 4 mm to 1 mm gradient thickness, curved freeform lightguide (nearly 4x thinner than the original freeform prism), and 2) lightguide fabrication utilizing ophthalmic machines. This particular optical design makes combined use of total internal reflections and partial reflections. The advantages of this optical architecture include the curved optical surfaces that eliminate the optical collimator requirement in flat lightguides, a relatively large eyebox, and a manufacturing approach that reuses the standard ophthalmic process for fabricating the eyeside and worldside optical surfaces. The limitations of the optical design are low efficiency ($\sim 5\%$), multiple image artifacts, and lack of optical see-through.

Keywords: Eyewear displays, freeform optics, ophthalmic fabrication

1. INTRODUCTION

Organized spatially, there are 3 possible configurations in the optical design space of mobile augmented reality displays as shown in Fig. 1.[1] All of these spatial choices are typically implemented as magnifiers due to their compactness compared to pupil-forming systems. The first option is to place the microdisplay and the optics in front of the eyewear lens. Google Glass is an example for option 1. The second option is to place the optics and the microdisplay behind the eyewear lens. The head-worn display optics literature is rich with examples using this option. The third option is to use the eyeglass lens itself as a magnifier. In this third category, optical lightguides are being explored as candidate architectures to solve the mobile optical see-through augmented reality display problem among other candidate architectures. Both flat and curved lightguides are being explored. Flat lightguides require a collimator optic that takes up volume, weight, and increases the complexity of the system. The classical freeform prism can be considered to be a curved lightguide. The classical freeform prism is approximately 18 mm thick and makes use of one total internal reflection. The original design form was published by Yamazaki et al. in 1999.[2] A thinner curved lightguide in this category is the technology developed at Tooz technologies.[3] Optical designs in the third option can be viewed as descendants of the freeform prism. In this paper we present the design and fabrication of a thin curved lightguide. The optical power in curved lightguides eliminate the collimator optic requirement as we demonstrate in this paper.

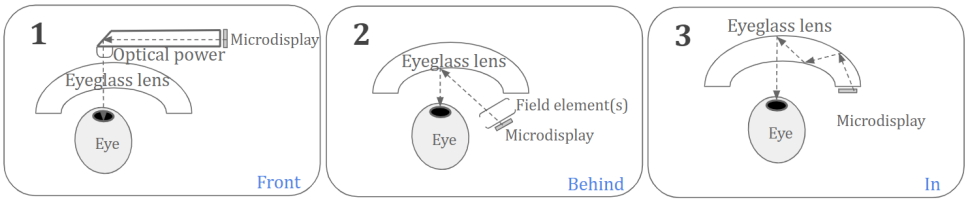

Figure 1: Spatial organization of eyewear display optics.

Correspondence author: ozancakmakci@google.com

Digital Optical Technologies 2019, edited by Bernard C. Kress, Peter Schelkens, Proc. of SPIE
Vol. 11062, 110620H · © 2019 SPIE · CCC code: 0277-786X/19/$21
doi: 10.1117/12.2530526

2. OPTICAL DESIGN

The optical design goal here is to come up with an optical magnifier geometry that uses existing optical surfaces of an eyeglass lens. Therefore, the geometry is severely constrained by the packaging requirements, specifically the worldside radius of curvature and the thickness of the final solution. Furthermore, we constrain the manufacturing of the design to existing eyewear manufacturing techniques (i.e., cast semi-finished puck, machine, polish, and edge). We describe an optical design that meets these constrains and has 5 bounces on the eyeside surface, and 6 bounces on the worldside surface. The thickness of the lightguide is 4 mm on the microdisplay side and down to approximately 1 mm on the thin side. The length of the lightguide is approximately 35 mm. Depending on the refractive index of the lightguide, a number of those bounces will total internally reflect and a number of those bounces will partially reflect. The optical layout is shown in 2. The eyeside and worldside surfaces are freeform surfaces. The incoupler surface facing the microdisplay is flat. The freeform surfaces are mathematically represented using x-y polynomials. The construction parameters are disclosed in our patent.[4] As shown in Fig. 3, >30% as-designed MTF margin (Nyquist set to 15μm pixels) can be achieved with these surface choices in this geometry. The maximum distortion is <2% as shown in Fig. 4. The field is relatively flat with < 0.25 diopter field curvature. We summarize additional example achievable design parameters in Table 1.

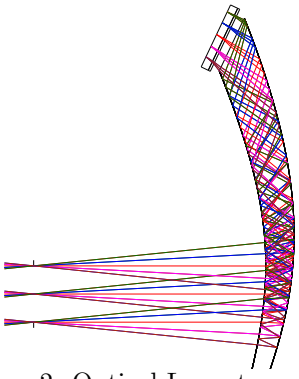

Figure 2: Optical Layout

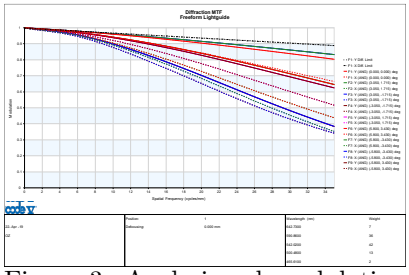

Figure 3: As-designed modulation transfer (Nyquist set to 15 micron pixels). Evaluated with a 5 mm centered pupil. The as-designed resolution in visual space is 1.2 arcminutes.

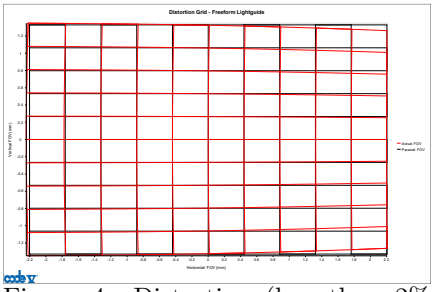

Figure 4: Distortion (less than 2% maximum distortion)

Table 1: Example achievable optical specifications with the design form.

Parameter	**Example achievable value**
Wavelengths [nm]	642.73, 590.86, 542.02, 500.48, 465.61
Diagonal FOV [deg]	15
Display diagonal [in]	0.26
Unvignetted circular pupil diameter [mm]	5
Eyerelief to cornea [mm]	15
Number of freeform surfaces	2
Optical material	Zeonex E-48R
As-designed MTF [35 cyc/mm]	> 30%
Distortion [%]	1.4
Telecentricity [deg]	2
Field curvature [diopters]	<0.25
Efficiency with 80% eyeside coating [nits/mW]	2
Active area dimensions [mm]	4.5 by 2.5
Square microdisplay pixel dimension [μm]	15

The optical performance is limited by variation of astigmatism with color as shown in Fig. 5. The astigmatism across the field of view is shown in Fig. 6.

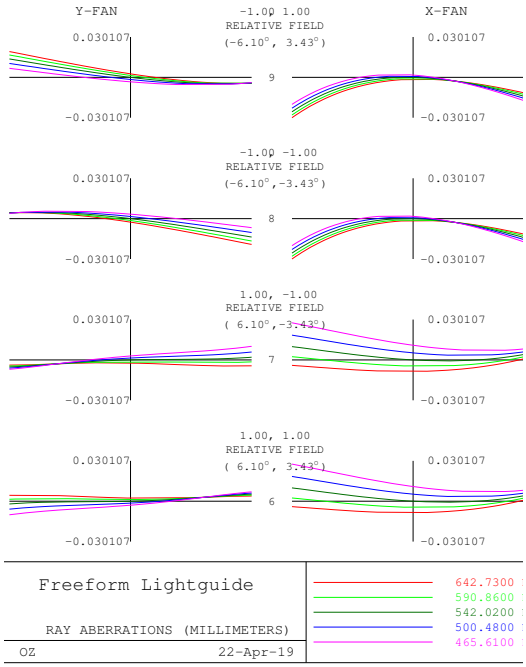

Figure 5: Transverse ray aberration plot at the edges of the field. The system is limited by lateral color and variation of astigmatism with color. Evaluated with a 5 mm diameter circular pupil.

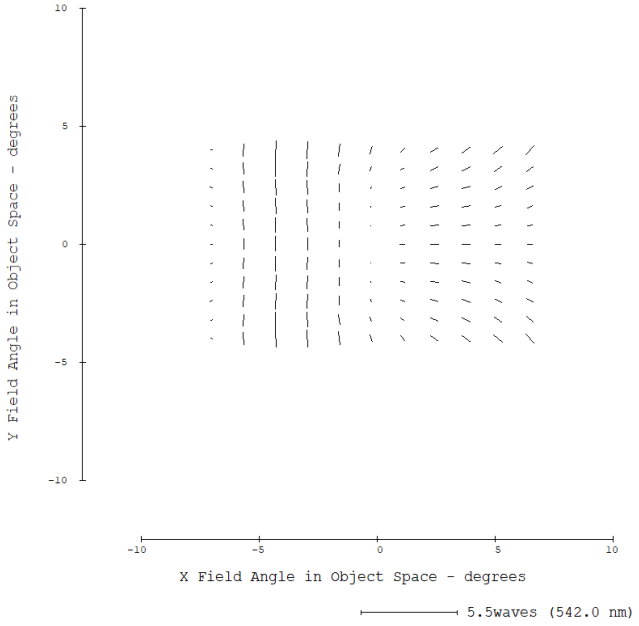

Figure 6: Astigmatism across the field. Notice the binodal astigmatism behavior within the rectangular field of view.

2.1 As-built performance

The modulation transfer functions at three orientations (0,45,90) after the tolerances listed in Table 2 are applied to the system are shown in Fig. 7a, 7b, 7c. The design with two freeform surfaces is sensitive to the assumed tolerances, primarily the 2 micron PV astigmatic surface figure error. A 4 arcminute resolution solution may be more realistic with this architecture. In the section on ophthalmic machining, we present metrology data that suggests consistently better PV numbers for spherical surfaces using these techniques. Characterizing PV surface figure numbers for freeform surfaces using these machines requires more process development work.

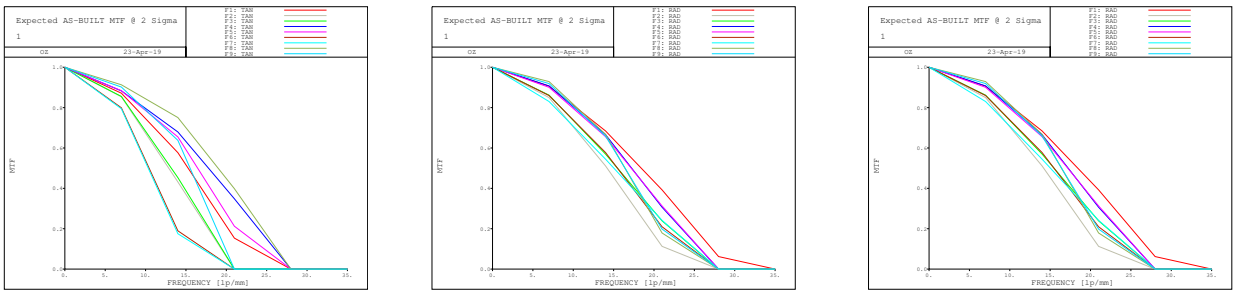

(a) As-built MTF tangential orientation. (b) As-built MTF radial orientation. (c) As-built MTF 45° orientation.

Figure 7: As-built MTF at 0, 45, and 90 degree orientations.

Table 2: List of tolerances assumed for the as-built MTF simulation.

Tolerance	**Value**
Peak-to-valley irregularity [um]	2
Surface tilt [°]	±0.1
Surface decenter [μm]	±15
Index	±0.001
Abbe [%]	±1
Compensator	Focus and microdisplay tilt

2.2 Eyebox

Our method of 3D eyebox analysis is described in an earlier paper.[5] The eyebox volume is evaluated at 363 eye positions. There are three eyerelief planes (nominal and 10 mm away and towards the optic). The lateral sampling for each eyerelief plane was 11 x 11 eye positions. The extent of lateral sampling was set to ±10 mm. As expected the eyebox volume shrinks as we go away from the optic and it gets larger as we get closer to the optic. A 5 point test pattern was used for the eyebox simulation. Each source was 100 μm^2 in dimension. The emission cone of the source was set to ±30° full width half-max (symmetric along two directions). The human eye is modeled as a 17 mm focal length perfect lens. The pupil diameter is set to 4 mm in diameter. The criterion for eyebox is nonuniformity across the 5 test points (i.e., $\frac{max-min}{max+min}$). Eyeroll is not taken into account in the eyebox simulations. The relevant portion of a nonuniformity slice from this 3D eyebox run at the nominal eyerelief plane is shown in Fig. 8a as a heatmap. The x and y axis of the heatmap correspond to the (x,y) location of the pupil relative to the nominal eyerelief position (at z=0), and the value in the heatmap is the nonuniformity of the 5 sources as viewed through the optics. In Fig. 8b, we show the isosurface enclosing the 3D eyebox volume for nonuniformity isocontours at a 70% threshold value. The resulting red surface is the eyebox surface enclosing the eyebox volume. As long as the center of the pupil is within this red eyebox surface, a user can view the virtual magnified image and the image will have 70% nonuniformity or less. Lower nonuniformity values are desirable, zero being ideal, one meaning that at least one of the source points clipped when viewed through the optic at that eye location.

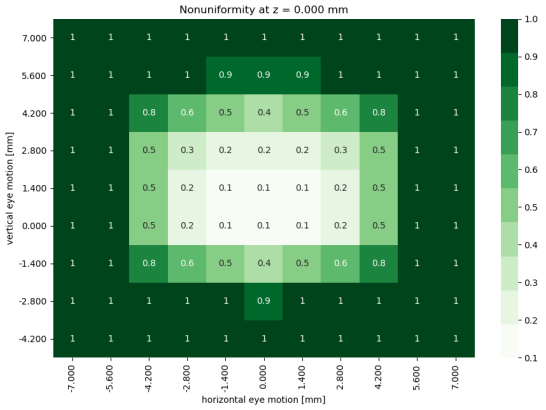

(a) Relevant portion of the nonuniformity heatmap at nominal eyerelief. The spatial sampling range is ±10mm. Horizontal eye motion of ±7 mm and vertical eye motion of +7 mm and −4.2 mm are shown.

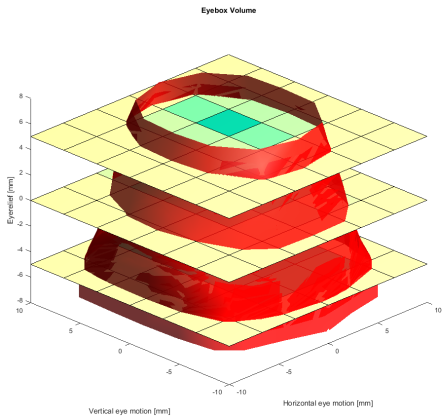

(b) Red surface encloses the eyebox volume.

Figure 8: 3D eyebox characterization based on nonuniformity criteria.

2.3 Material Selection

Choice of optical plastic, as opposed to glass, makes the design suitable for fabrication using standard ophthalmic machines as we discuss later in the paper. However, plastic would yield lower optical efficiency because high index optical plastics have a larger critical angle compared to high index moldable glasses. Glass designs would be more optically efficient. A moldable high index glass would be required if the design is implemented in glass. It is unlikely that the design would pass the ball drop test if the material choice was glass. High index plastics combined with the curvature of the lightguide allows two of the bounces close to the microdisplay to be in total internal reflection, and the rest for bounces are in partial reflection.

2.4 Efficiency and Coatings

In Zeonex E-48R ($n_d \approx 1.53$), the critical angle is approximately 40.8 degrees. In Fig. 9a, we list the angles of incidence on worldside and eyeside surfaces. The angles of incidence on the worldside are 59.9°, 49.3°, 38.5°, 27.6°, 16.5°, 5.2°, in the order of light propagation from the source to the eye. The angles of incidence on the eyeside surface, in the order of light propagation from the source to the eye, are 56.9°, 47.4°, 35.5°, 23.5°, 11.43°, 0.6°. The main point is that, with this material and geometry choice, two of the bounces are in total internal reflection, and four of the bounces are partial reflections on the worldside. The optical efficiency as a function eyeside and worldside coatings is shown in Fig. 9b. The optimum efficiency is achieved with a full mirror worldside and $\sim 75\%$ eyeside reflectivity.

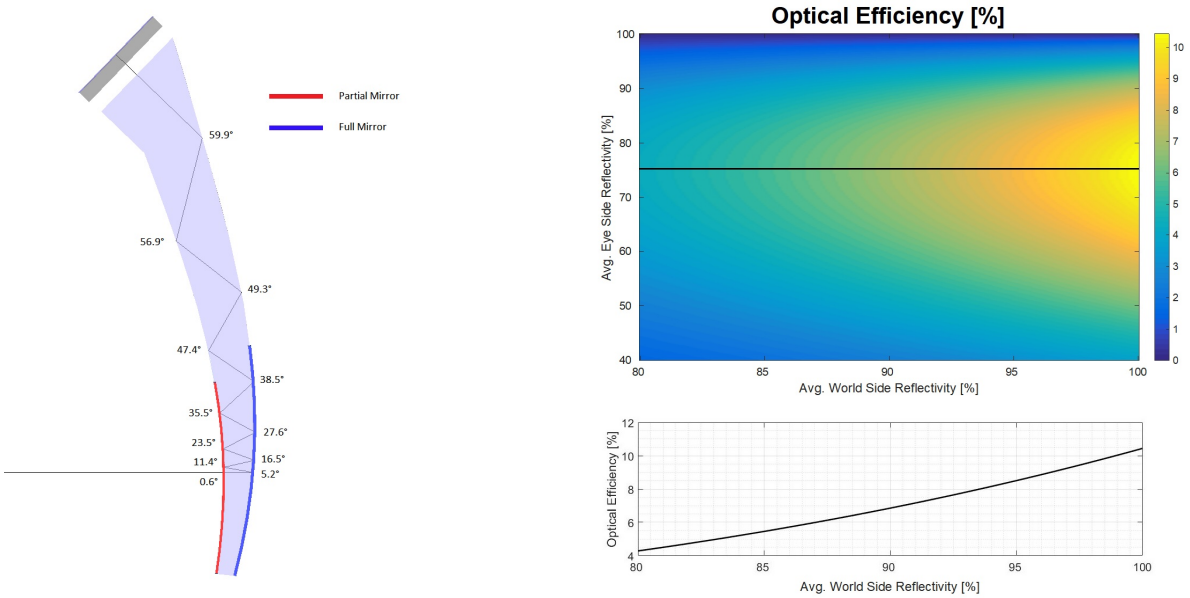

(a) Chief ray trace showing angles of incidence on eyeside and worldside surfaces.

(b) Optical efficiency as a function of eyeside and worldside coating reflectivities.

Figure 9: Choice of optimum coating reflectivities to maximize efficiency.

2.5 Artifacts

In Fig. 10, we show that a simulation of an eye rotated by +/-5 degrees causes side images to appear. The luminance of the side images will depend on the coating configuration. A pure horizontal shift of the eye (+/-4mm) along the IPD dimension does not cause side images as shown in Fig. 11.

2.6 Concept design

The main design concept here originates from pursuing the question of what optical architectures could we design while reusing the standard opthalmic fabrication channels as they exist today. In addition, the specific curved

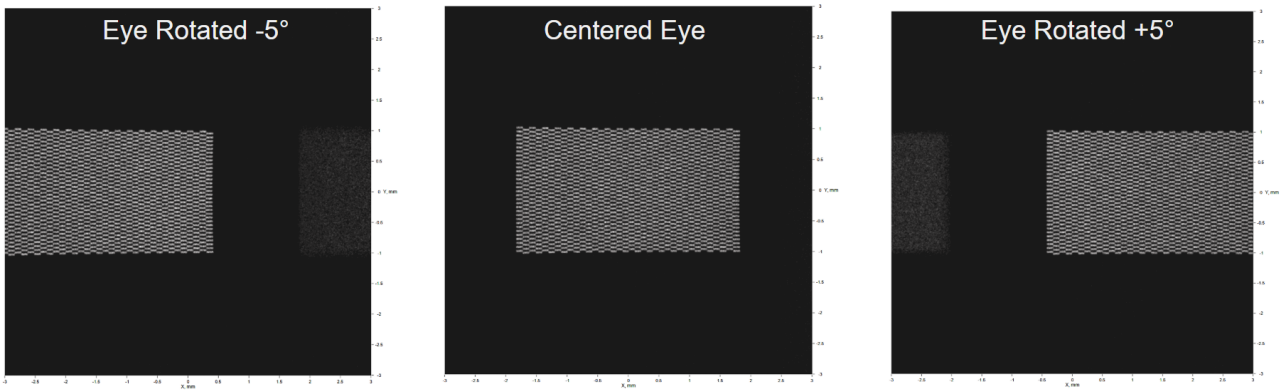

Figure 10: Side images appear as the eye is rotated 5 degrees away from the main images. Three simulations are shown for the cases of -5 degree rotation, no rotation (baseline), and +5 degree rotation.

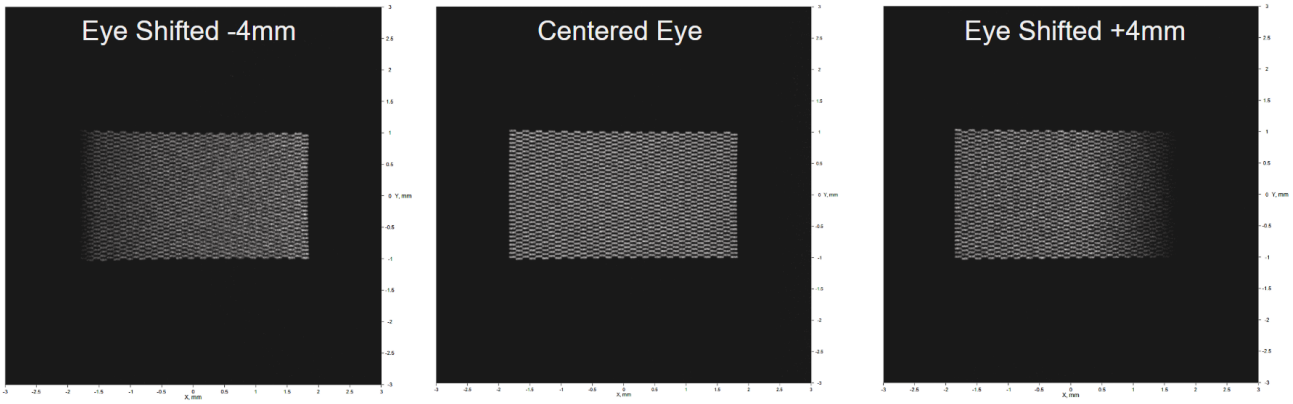

Figure 11: Three simulation results are shown for the cases of a horizontal shift of -4 mm, no shift (baseline), and +4 mm shift of the eye.

lightguide approach here follows the shape of the frame, while maintaining thin temples. To that end, prescription eyewear today has two optical surfaces. An eyeside optical surface and a worldside optical surface. The design presented here makes use of three optical surfaces. Two of those optical surfaces can be generated with existing ophthalmic equipment. The third optical surface, in the simplest implementation, is a flat surface. Even though we did not validate the fabrication of the third optical surface using the standard ophthalmic design flow, we believe that edging and polishing maybe reused to fabricate the entire design using the ophthalmic process. Note that edges of eyewear are already polished in the standard process today to obtain an improved finish. The design is conducive for implementation of a hinge. A thin curved lightguide integration concept into eyewear is shown in Fig. 12a. A frontal view of the lightguide integrated into eyewear is shown in Fig. 12b.

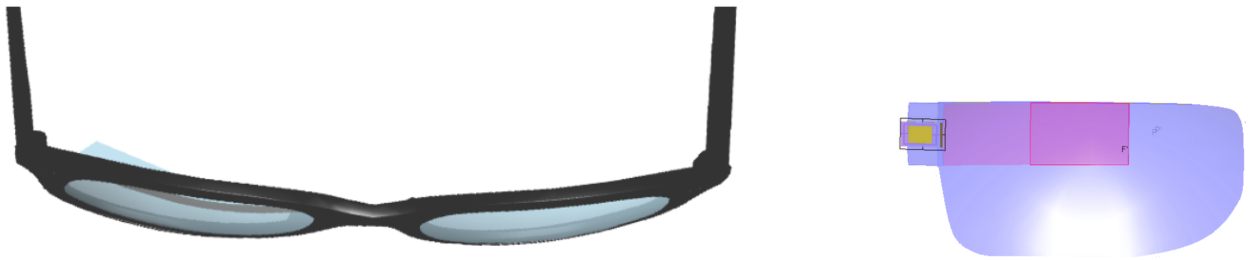

(a) Top view. (b) Front view.

Figure 12: Concept design illustration of lightguide integration in eyewear.

2.7 Image location

The image location shown in this design is coincident with line of sight. As the optical design shown here is not see-through, a redesign would be required to move the optics above the line of sight so that the worldside sphere is maintained while the optics is moved and the image is seen when the user glances up, similar to Google Glass. An illustration of what it would mean to do move the image above line-of-sight is shown in Fig. 12b. The purple region would not be optical see-through due to the lightguide. The blue region would remain see-through.

3. CURVED LIGHTGUIDE MANUFACTURING USING OPHTHALMIC MACHINES

Ophthalmic machines are typically not used for fabricating optics other than eyewear optics. To our knowledge, this is the first report of a lightguide being fabricated using standard ophthalmic fabrication techniques. We summarize and introduce the main process steps in fabrication using ophthalmic machines. This process is the fastest rapid prototyping technique that we are aware of that is capable of producing large area optical quality surfaces suitable for lightguide fabrication. Compared to diamond turning or milling that requires hours of finishing time, and many more hours for setup time (i.e., preparing jigs to hold the part, writing custom g-code, obtaining custom diamond tools, and so on), a typical ophthalmic lens is produced on the order of 1 minute. 3D printing is not as fast or mature enough at the time of this writing to deliver the surface figure and slope characteristics that can be achieved with ophthalmic machines today. The ophthalmic process is a mass manufacturing process as this process is used in the eyewear industry today.

The standard ophthalmic process available today can incorporate freeform optical surfaces for the eyeside surface in mass production. The main steps involved in ophthalmic fabrication flow are shown in Fig. 13. There are several additional steps, however, there are textbooks on the subject that cover this topic in more detail. For an in-depth discussion of the ophthalmic process, see Brooks.[6] Tolerance recommendations for refractive power, cylinder axis, base curve, center thickness, and so on are discussed in ANSI Z80.1.[7]

The fact that this optical design is close to eyewear thickness and it is composed of 3 optical surfaces make it close to being compatible with manufacturing using ophthalmic machines.

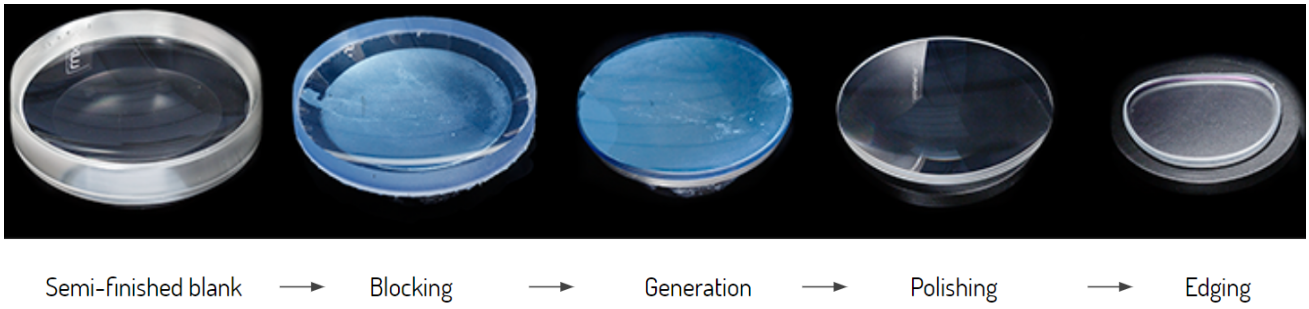

Figure 13: Simplified ophthalmic process flow steps: semi-finished blank, blocking, generation, polishing, and edging. This simplified summary ignores lens protection, measuring, laser marking, deblocking, tape stripping, tinting, hard coating, and AR-coating steps.

3.1 Semi-finished blank

The process starts with the selection of a blank with appropriate material. Typical ophthalmic materials include CR-39 ($n_d = 1.498, \nu = 59.3$), polycarbonate ($n_d = 1.586, \nu = 30$), trivex ($n_d = 1.532, \nu = 44$), as well as high index options, for example, Mitsui MR-174 ($n_d = 1.74, \nu = 33$). The worldside optical surface is used as-is from a casted ophthalmic puck.

3.2 Blocking/Deblocking

Blocking is the concept of holding the semi-finished lens material during surfacing. A number of methods for blocking have been developed including low-temperature-melting alloys (between 45°C and 60°C). The standard ophthalmic pucks are larger than the material used in eyeglasses and when they are blocked, they have considerable overhang. Cribbing is the process of removing overhang from the ophthalmic puck. Deblocking is the step where the alloy gets removed from the lens. In terms of alloy material choices, the industry has been moving towards environmental friendly materials that avoid cadmium and lead for example.

3.3 Generation

The process of cutting the desired eyeside optical surface is called generation. In prescription glasses, the worldside optical is typically kept as-is from the semi-finished ophthalmic puck. In optical design of thin curved lightguides, an optical designer may choose to reuse the worldside radius of curvature from a standard puck or customize both eyeside and worldside optical surfaces. In any case, the surface from the output of the generation step is not yet an optical surface. The generation process takes less than one minute making it applicable to mass production as well as an excellent rapid prototyping tool. Essentially, the sag ($z = f(x, y)$) of a surface is written as a surface definition file (SDF) and this format can readily be used to communicate an optical design with generators.

3.4 Polishing

Toolwear and chips during generation influence the surface figure. Therefore, polishing is typically required in order to obtain an optical finish. We measured PVr of 28 optical surfaces generated and polished using the ophthalmic process and we find the an average PVr of 1.4 microns (standard deviation of 0.48 microns) to be achievable with an average 103.5 microradian slope error (standard deviation of 16.9 microradians). Note that these PVr values are for a subaperture of approximately 30 mm x 10 mm. A representative sample interferogram for a polished surface is shown in Fig. 14 for a 55 mm diameter aperture.

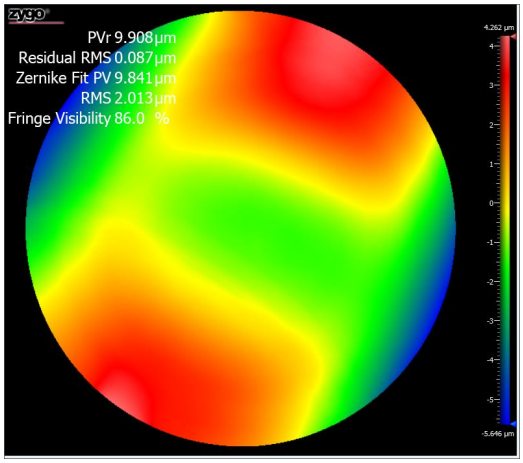

Figure 14: Interferogram of a sample generated and polished surface. This particular example generated and polished surface has PVr of 9.9 μm across a 55 mm diameter ($R_q \sim 10$ nm).

3.5 Edging

The cribbed lens size is closer to the edged lens size. The relationship between a semifinished blank, a cribbed contour, and an edged lens size is illustrated in Fig. 15. Edging is the fabrication process of milling the cribbed lens to have the contour curve for the target frame. Tracers can be used to extract the edging contour from a target frame.

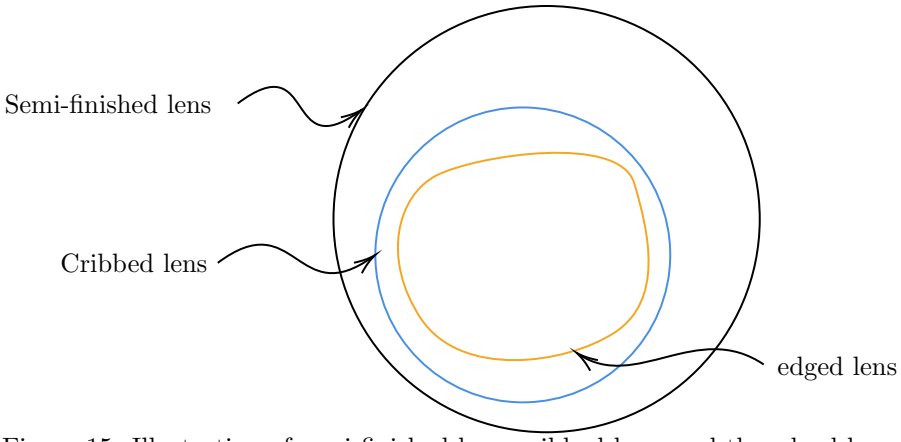

Figure 15: Illustration of semi-finished lens, cribbed lens, and the edged lens.

4. RESULTS FROM THE INITIAL PROTOTYPE

A version of the presented design was fabricated using the standard ophthalmic process. Specifically, one having a flat incoupler surface, a spherical worldside surface, and a freeform eyeside surface. The spherical surface reuses the casting radius of 84.94 mm from a semi-finished ophthalmic puck. The material for the starting point blank was Trivex. One of the fabricated testcase samples are shown while it is on the blocker in Fig. 16. The generated, polished, and deblocked optic is shown in Fig. 17. The testcase optic in the measurement setup is shown in Fig. 18. We used an uncoated optic to get test images. This requires a high luminance source to get an image. We used a 260k nit compact backlight illuminating a film to acquire a testimage. The backlight and film are shown in Fig. 19. A magnified image of the backlight and film as seen through the optic is shown in Fig. 20. If we place the camera close to the optic, it was possible to capture the partial reflections as they propagate through the lightguide and form images, as shown in Fig. 21.

Figure 16: Testcase optic on blocker

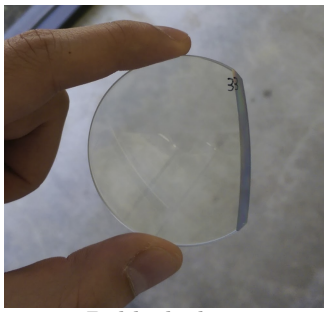

Figure 17: Deblocked testcase optic after generation and polishing

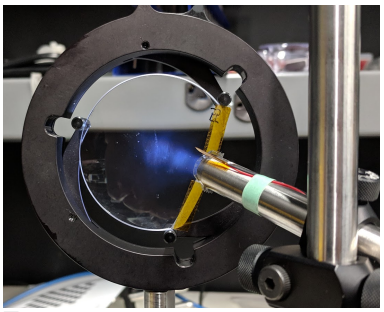

Figure 18: Testcase optic measurement setup

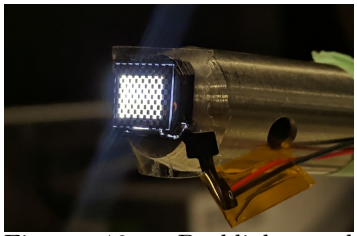

Figure 19: Backlight and checkboard test target

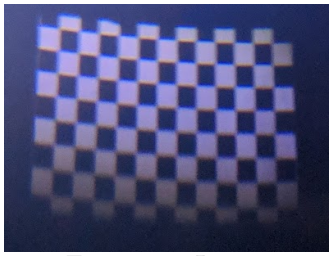

Figure 20: Image

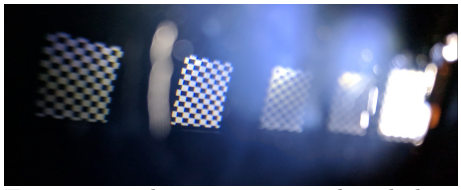

Figure 21: The camera was placed close to capture the partial reflection bounces from the optic.

5. CONCLUSION

We designed and fabricated a thin curved optical lightguide that is suitable for integration in eyewear optics. The design makes combined use of total and partial internal reflections and yields a configuration that is 4x thinner than the original freeform prism. The thickness portion of the optic is 4 mm down to approximately 1 mm. The design is composed of 3 optical surfaces making it applicable for manufacturing using standard ophthalmic equipment. That is, two of the optical surfaces can be readily manufactured using standard opthalmic machines. The third surface, depending on the surface type, may be cut using an edger and then polished. The testcase we fabricated has a flat incoupling surface that was cut using a flycutter. The advantages of this optical architecture include the curved optical surfaces that eliminate the optical collimator requirement in flat lightguides, a relatively large eyebox, and a manufacturing approach that reuses the standard ophthalmic process for fabricating the eyeside and worldside optical surfaces. The limitations of the optical design are low efficiency at $\sim 5\%$, multiple image artifacts, and lack of optical see-through.

REFERENCES

[1] Spitzer, M. B., "18.4: Invited paper: Development of eyewear display systems: A long journey," in [*SID Symposium Digest of Technical Papers*], **45**(1), 230–233, Wiley Online Library (2014).

[2] Yamazaki, S., Inoguchi, K., Saito, Y., Morishima, H., and Taniguchi, N., "Thin wide-field-of-view hmd with free-form-surface prism and applications," in [*Stereoscopic Displays and Virtual Reality Systems VI*], **3639**, 453–463, International Society for Optics and Photonics (1999).

[3] "Tooz technologies website." https://www.tooztech.com/. Accessed: 2019-02-23.

[4] Cakmakci, O. and Gupta, A., "Eyepiece for head wearable display using partial and total internal reflections," (July 12 2016). US Patent 9,389,422.

[5] Cakmakci, O., Hoffman, D., and Balram, N., "31-4: Invited paper: 3d eyebox in augmented and virtual reality optics," in [*SID Symposium Digest of Technical Papers*], **50**(1), Wiley Online Library (2019).

[6] Brooks, C. W., [*Essentials of Ophthalmic Lens Finishing*], Elsevier Health Sciences (2003).

[7] "Ophthalmics - Prescription Ophthalmic Lenses - Recommendations," ansi z80.1 standard, American National Standards Institute (2015).